論文 10-3-15

직접분사 엔진의 유동장 및 분무특성에 미치는 선회비의 영향에 대한 수치해석적 연구

Numerical Simulation of Swirl Effect on the Flow Fields and Spray Characteristics in Direct Injection Engine

홍 기 배*·김 형 섭*·양 희 천**·유 홍 선**
K. B. Hong·H. S. Kim·H. C. Yang·H. S. Ryou

ABSTRACT

Since the rate and completeness of combustion in direct injection engines were controlled by the characteristics of gas flow fields and sprays, an understanding of those was essential to the design of the direct injection engines. In this study the numerical simulations of swirl effects on the characteristics of gas flow fields and sprays were performed using the spray model that could predict the interactions between gas fields and spray droplets. The governing equations were discretized by the finite volume method and the modified k-ε model which included the compressibility effects due to the compression/expansion of piston was used.

The results of numerical calculation of the spray characteristics in the quiescent environment were compared with the experimental data. There were good agreements between the results of calculation and the experimental data, except in the early stages of spray.

In the motoring condition, the results showed that a substantial air entrainment into the spray volume was emerged and hence the squish motion was relatively unimportant during fuel injection periods. As the swirl ratio increased, the evaporation rate was increased due to the wide dispersion of the spray droplets and the strong interaction between spray droplets and gas fields.

국문요약

직접분사엔진에서 기상과 분무액적간의 유동특성 및 분무특성에 미치는 선회비의 영향에 대하여 수치해석하였다.

정적인 환경에서는 분무초기를 제외하고는 계산과 실험결과가 잘 일치하였다.

운전상태에서는 연료분사 기간동안 속도장의 영향이 증가하여 스퀴시유동의 중요성이 상대적으로 감소하였다.

선회비가 증가할수록 높은 난류에너지가 연소실내에 분포되며 분무액적이 확산되고 기상과의 상호작용이 강해져서 증발률이 증가하였다.

1. INTRODUCTION

In the direct injection engines fuel was injected by the fuel-injection system into the combustion chamber toward the end of compression stroke. The injected fuel was vaporized and mixed with the high-temperature compressed air and then spon-

* 아주대학교 기계공학과
** 중앙대학교 기계공학과

taneous ignition of portions of the premixed fuel and air occurred after a delay period. However the combustion of direct injection engine was a intrinsically heterogeneous diffusive combustion, it caused an air pollution due to the production of soot in a combustion region of locally dense fuel-air mixture. Therefore a number of studies of the characteristics of flow and fuel spray in a combustion chamber have been performed in order to decrease air pollutants and increase the combustion efficiency. Since the spray characteristics of an injected fuel governed the fuel-air mixing rate and could control combustion process, experimental and numerical studies of spray characteristics have been performed extensively. The experimental studies of spray characteristics were initiated from the study of single droplet and were extended to the motoring condition of the direct injection engine. Since the experimental studies of spray characteristics in an motoring condition of diesel engine were extremely difficult, most results have come from the studies of fuel injection into constant-volume chambers filled with the high-pressure quiescent air at the room temperature. For this reason, most experimental studies were restricted to the measurements of spray tip penetration, spray angle and droplets size distribution in a quiescent environment[1~3].

Until recently, the detailed numerical studies of practical sprays were impossible due to the complexity of physical process and the problems of computer storage and performance. The first step toward the numerical studies of practical spays was taken when a statistical formulation was proposed for the spray analysis. The spray was discretized into computational droplets that followed droplet characteristic paths and was handled by solving the Lagrangian equations for the motion of individual droplets passing through the gas phase. Each droplet was considered to represent a 'parcel' of spherical non-interacting droplets having the same size, velocity, temperature, etc.

In an important advance of numerical methods for sprays, Dukowicz[4] suggested that the idea of the Monte Carlo method could be combined with droplet method for spray analysis. The major extension of the stochastic particle method was suggested by O'Rourke[5], who developed and applied a method for calculating droplet collisions and coalescence. Consistent with the stochastic particle method, collisions were calculated by a statistical approach rather than a deterministic approach. Also the major extension of the stochastic particle method was the recent addition by Reitz and Diwakar[6] of a method for calculating droplet breakup. An alternative model for droplet breakup based on an analogy, suggested by Taylor[7], between an oscillating and distorting droplet and a spring-mass system was suggested, which was called TAB method[8].

Fuel sprays might impinge on the piston bowl and crown in DI diesel engine and might have a great influence on the mixture formation and the combustion process. It made the liquid fuel concentrated at the impingement site and reduced the fuel evaporation. Thus several approaches have been used in multidimensional models to account for droplet impingement on a solid wall[9~11].

The fuel was dispersed in the form of droplets and that there were fuel-rich and fuel-free zones in the combustion chamber of the direct injection engine. Whilst the small droplets approaching the wall were deflected away, the large droplets struck the wall and then flowed along the wall surface. The effect of gas swirl was to spread the droplets of fuel-rich zones and the liquid layer over the surface. Generally in the direct injection engines as an engine size decreased, increasing amounts of air swirl were used to achive faster fuel-air mixing rates. But few numerical studies of swirl effect on the spray characteristics were made[11~13].

In this study the numerical calculations of the swirl effects on the spray characteristics and the flow fields in a motoring condition of direct injection engine were performed using the spray model that could predict the interactions between spray droplets and gas fields. That model accounted for

the effects of droplet evaporation, droplet breakup, droplet collision and coalescence and the effect of droplets on the gas turbulence. And the numerical calculations of the spray characteristics in a quiescent environment were performed and were compared with the experimental data[14].

2. MATHEMETICAL MODEL

2.1 Goverming equations

The gas phase conservation equations were written in ensemble averaged form with density-weighting being applied to account for density variation due to the compressibility effects. The turbulent gas phase flow was modelled using the modified k-ϵ model accounting for bulk compressibility effects due to the rapid compression/expansion[15]. The transport equations for mass, momentum, specific energy, fuel vapor mass fraction, turbulence kinetic enrgy and its dissipation rate for the gas phase could all be written in the general form

$$\frac{1}{\Delta V}\frac{\partial}{\partial t}(\theta\rho\Delta V\psi)+\frac{\partial}{\partial\zeta}(\theta\rho w_R\psi)+\frac{1}{\Delta\eta}\frac{\partial}{\partial\xi}(\theta\rho\Delta\eta u\psi)+\frac{1}{\Delta\xi}\frac{\partial}{\partial\eta}(\theta\rho\Delta\xi v\psi)=\frac{\partial}{\partial\zeta}\left(\theta\Gamma_\psi\frac{\partial\psi}{\partial\zeta}\right)+\frac{1}{\Delta\eta}\frac{\partial}{\partial\xi}\left(\theta\Gamma_\psi\Delta\eta\frac{\partial\psi}{\partial\xi}\right)+\frac{1}{\Delta\xi}\frac{\partial}{\partial\eta}\left(\theta\Gamma_\psi\Delta\xi\frac{\partial\psi}{\partial\eta}\right)+S_\psi+S_\psi^d \quad \cdots\cdots (1)$$

Where $\Delta V=\Delta\xi\Delta\eta\Delta\zeta$ was the local incremental volme whose sides had arc lengths $\Delta\xi$, $\Delta\eta$ and $\Delta\zeta$ and w_R was the axial gas velocity relative to the moving grid. The diffusion coefficients τ_ψ and source terms S_ψ were defined in the Ref.[16]. The source terms with superscript d came from interactions with the liquid phase and were given by

$$S_m^d=-\frac{\pi\rho d}{6V\delta t}\sum_k N_k\{(D_{d,k}^n)^3-(D_{d,k}^o)^3\}$$

$$S_u^d=-\frac{\pi\rho d}{6V\delta t}\sum_k N_k\{(D_{d,k}^n)^3U_{d,k}^n-(D_{d,k}^o)^3U_{d,k}^o\}$$

$$S_e^d=-\frac{\pi\rho d}{6V\delta t}\sum_k N_k\{(D_{d,k}^n)^3(C_vT_{d,k})^n-(D_{d,k}^o)^3(C_vT_{d,k})^o\} \quad \cdots\cdots (2)$$

where N_k is the number of droplet in parcel k.

Following Dukowicz[4] the liquid phase was modelled using the stochastic method. The droplet equations of motion were written in Lagrangian form, thus the droplets could be tracked in time as they passed through the gas phase. The droplet trajectory and momentum equations were written as follow;

$$\frac{d\xi_d}{dt}=u_d,\quad \frac{d\eta_d}{dt}=v_d,\quad \frac{d\zeta_d}{dt}=w_d \quad \cdots\cdots (3)$$

$$\frac{du_d}{dt}=K_d(u_g+u'_g-u_d)+S_{ud}$$

$$\frac{dv_d}{dt}=K_d(v_g+v'_g-v_d)+S_{vd} \quad \cdots\cdots (4)$$

$$\frac{dw_d}{dt}=K_d(w_g+w'_g-w_d)+S_{wd}$$

The evaporation of the droplets were calculated by solving the Lagrangian fuel mass and energy conservation equations. Thus

$$\frac{dm_d}{dt}=-\pi D_dDP_t\ln\left(\frac{P_t-P_{v,\infty}}{P_t-P_{v,s}}\right)Sh/RT_m \quad \cdots\cdots (5)$$

$$\frac{d(mC_pT)_d}{dt}=\pi D_dk_t(T_g-T_d)\left(\frac{z}{e^z-1}\right)Nu+Q\frac{dm_d}{dt} \quad \cdots\cdots (6)$$

The major models used for droplet interactions were the collision and coalescence model of O'Rourke[5], and the droplet breakup model of Reitz and Diwaker[6].

2.2 Boundary and initial conditions

A number of gas phase boundary conditions need to be applied to the calculation. The wall-function method of Launder and Spalding[17] was employed. At the valve inlet, the mass flow past the valve was modelled as that of quasi-steady isentropic flow through an orifice. The average properties within

the cylinder were given by the following equations.

orifice flow : $m_{in}=a_{in}C_D(2\rho_{in}\Delta P)^{1/2}$ ····· (7)

overall continuity : $\frac{dm_{cyl}}{dt}=\dot{m}_{in}$ ····· (8)

overall energy : $\frac{dH_{cyl}}{dt}=V_{cyl}\frac{dP_{cyl}}{dt}+\left(h_{in}+\frac{u^2_{in}}{2}\right)\dot{m}_{in}+\sum_i \alpha_i(T_{wi}-T_{cyl})a_{wi}$ ····· (9)

equation of state : $P_{cyl}=R\rho_{cyl}T_{cyl}$ ····· (10)

where m, H, h, T, P were gas phase mass, enthalpy, specific enthalpy, temperature, pressure.

The atomization process was not modelled, rather the spray was assumed to be fully atomized whilst crossing one computational cell which was called the injector cell. It was assumed that the injection direction made an angle α_z with the cylinder axis, as shown in Fig. 1, and an angle α_x with the x axis of the grid, defined to be the J=2 grid line. Further it was assumed that the radial-like grid lines of the injection cell made an angle α_g with the x axis. Then the injection velocity vector was given by

$\underline{V}_{inj}=(U_{inj}\sin\alpha_z\cos(\alpha_x-\alpha_g),\ U_{inj}\sin\alpha_x\sin(\alpha_x-\alpha_g),\ U_{inj}\cos\alpha_z)$ ····· (11)

and U_{inj} was given by

$$U_{inj}=C_o\left(\frac{2\Delta P}{\rho_d}\right)^{0.5} \quad \cdots\cdots (12)$$

where C_o was discharge coefficient, ΔP was difference between the injection pressure and the pressure of the combustion chamber and ρd was density of the droplets.

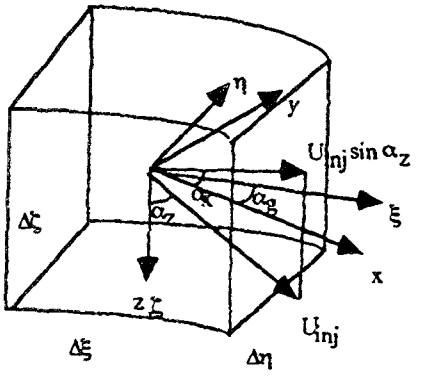

Fig. 1 The injection cell

3. SOLUTION METHOD

3.1 Grid system

The computational grid system which was generated analytically was illustrated in the plane view in the Fig. 2. A grid of variable axial spacing was used to allow for the change of the volume in the swept and clearance volume, while a fixed grid system was used for the region of the piston bowl.

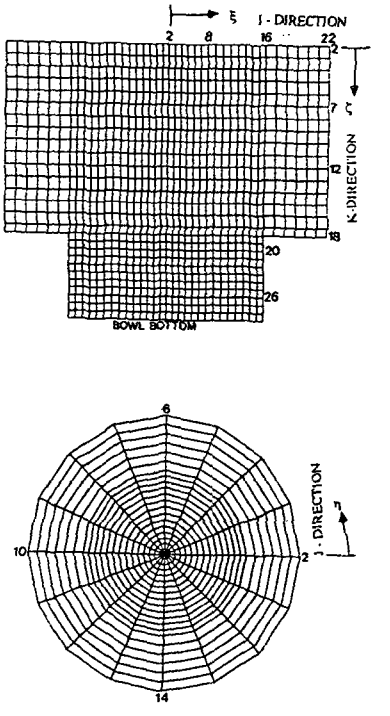

Fig. 2 Coordinate system and computational grid

3.2 The discretization

The finite volume method was used to transform the partial differential equations governing the gas phase flow into solvable algebraic equations. Here Euler implicit temporal discretization and a hybrid

scheme for spatial discretization were used. The finite volume momentum equations took the following form

$$A^n_p u^n_{g,p} = \Sigma A^n_m u^n_{g,p} + A^o_p u^o_{g,p} - \theta^n_p a \nabla P^n - \frac{1}{\delta t} \Sigma N_{d,k}(m^n_{d,k} u^n_{d,k} - m^o_{d,k} u^o_{d,k}) \quad \cdots\cdots (13)$$

As they were expressed in the Lagrangian form the droplet trajectory, momentum, mass and energy equations did not require a spatial grid in order to express them in algebraic form. The Lagrangian trajectory and momentum conservation equations of the ξ-direction were written in the Euler implicit finite difference form as

$$\xi^n_d = \xi^o_d + \delta t \cdot u^n_d \quad \cdots\cdots (14)$$

$$u^n_d = \frac{u^o_d + \delta t \cdot K^u_d (u^n + u^n) + \delta t \cdot S^n_{ud}}{1 + \delta t \cdot K^n_d} \quad \cdots\cdots (15)$$

The droplet mass and energy conservation equations were also expressed in the Euler implicit form as

$$m^n_d = m^o_d - \delta t \cdot \pi D^n_d \left\{ DP_t \ln\left(\frac{P_t - P_{v,\infty}}{P_t - P_{v,s}}\right) \frac{Sh}{RT_m} \right\}^n \quad \cdots\cdots (16)$$

$$(mC_pT)^n_d = (mC_pT)^o_d + \delta t \cdot \pi D^n_d (T^n_g - T^n_d) \left\{ k\left(\frac{z}{e^z - 1}\right) Nu \right\}^n + Q^n (m^n_d - m^o_d) \quad \cdots\cdots (17)$$

where T_d was the droplet temperature and T_g was local gas phase temperature.

3.3 The solution algorithm

Since the algebraic finite volume and finite difference equations were written in fully implicit form and PISO(Pressure Implicit by Splitting of Operators) algorithm was used[18].

4. RESULTS AND DISCUSSION

The numerical calculations of the spray characteristics in a quiescent environment and the swirl effect on the spray characteristics and the flow fields in a motoring condition were performed using the orthogonal curvilinear grid system and PISO algorithm. The results of calculations in the quiescent environment were compared with the experimental data[14] in order to validate the numerical method.

The grid systems and the engine specifications for calculation were shown in Fig. 2 and Table 1. The calculation was initiated at ATDC 90° being an intake stroke and was ended at ATDC 380° being an expansion stroke in a motoring condition. The crank angle increment was 0.25°(23.2 μs) for all calculations.

4.1 The spray characteristic in the quiescent condition

The cylinderical computational domain which had the specification as Table 1 was consisted of 20 radial, 20 circumferencial and 60 axial computational grids. An evaporation of the injection fuel was not considered because the temperatures of combustion chamber and injection fuel were equal at 300K.

The result of calculation of spray tip penetration being compared with the experimental data[14] were shown in Fig. 3. There were good agreement between the result of calculation and the experimental data, except in the early stages of the case of the nozzle diameter 0.2mm. The recent measuerments of electrical conductivity in the spray suggested that there was an 'intact core' of essentially unbroken liquid in the vicinity of the nozzle exit and the length of the core could be hundreds of nozzle diameters[19]. Hence that discrepancy in the stages of spray was attributed by the assumption that the spray was already atomized at the nozzle exit. In the spray model of this study the initial droplet sizes were specified assuming the normal distribution within the range 0<droplet diameter<injector nozzle diameter.

4.2 The swirl effect on the flow fields and the spray characteristics in the motoring condition

As shown in Fig. 3, the results of penetration length compared to the experimental data in the 3mm nozzle case was better than in the 2mm nozzle case. Hence the 3mm was used as the nozzle diameter.

The flow fields. Fig. 4 showed the velocity fields

Table 1 Engine specifications and calculation parameters quiescent condition

Bore[mm]	: 190
Stroke[mm]	: 450
Temperature of combustion chamber[K]	: 300
Temperature of injection fuel[K]	: 300
Pressure of combustion chamber[MPa]	: 2.0
Injection pressure[MPa]	: 10,40
Injection nozzle diameter[mm]	: 0.2,0.3

motoring condition

Engine speed[rpm]	: 1800
Bore[mm]	: 105
Stroke[mm]	: 108
Clearance[mm]	: 12
Piston bowl diameter[mm]	: 61.67
Piston bowl depth[mm]	: 22.76
Compression ratio	: 10
Initial temperature of combustion chamber[K]	: 550
Temperature of injection fuel[K]	: 300
Crank angle of injection start[deg]	: ATDC 341
Crank angle of injection end[deg]	: ATDC 359
Injection nozzle diameter[mm]	: 0.3
Injection pressure[MPa]	: 20

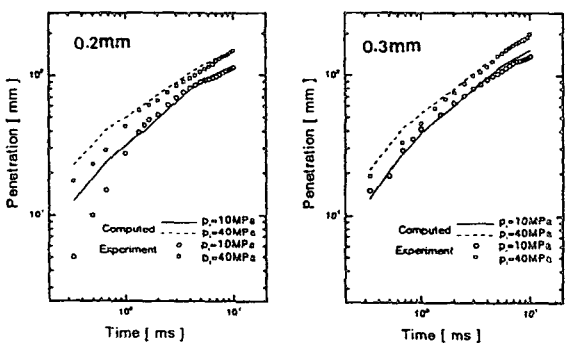

Fig. 3 Spray tip penetration versus time for nozzle diameter 0.2mm and 0.3mm

of the radial-axial plane in the case of swirl ratio 2. At ATDC 340° just before a fuel injection started, two toroidal vortices were revealed due to the strong squish motion produced by the pressence of bowl in squish region and bowl respectively. At ATDC 350° and ATDC 360° the velocity fields were strongly

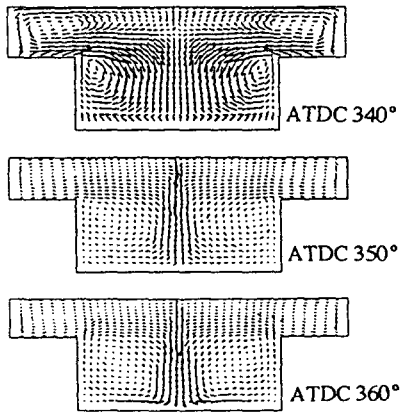

Fig. 4 Velocity fields in the plane of J=2 and J=10 u_{max}=8.79[m/s], w_{max}=54.54[m/s]

influenced by high pressure spray and the squish motion was relatively unimportant. A substantial air entrainment into the spray volume where it was accelerated in the direction of injection was emerged. The maximum velocities were between 5 and 7 times larger than those previous to the fuel injection at ATDC 340°. The velocity vectors being entrained by the spray had a dominant effect on the velocity fields near the axis of combustion chamber. The center of toroidal vortex in the bowl was shifted toward the axis of combustion chamber, although there remained substantially similar toroidal vortices in the same way at the ATDC 340°. But during the compression stroke the swirl effect on the change of velocity fields was appeared little in the radial-axial plane.

Fig. 5 showed the change of velocity fields in the radial-circumferential planes at ATDC 350° for different swirl ratios. In the plane of K=12 as a swirl ratio increased there revealed a solid-body rotation while as a swirl ratio decreased there revealed a spiralling motion that velocity vectors were concentrated toward the axis of combustion chamber. The spiralling was presumeably caused due to the concentration of the injected fuel in the vicinity of the the axis. In the plane of K=20 there revealed a spirlling motion and a irregular velocity vectors in the vicinity of the axis as swirl ratio decreased. The irregular

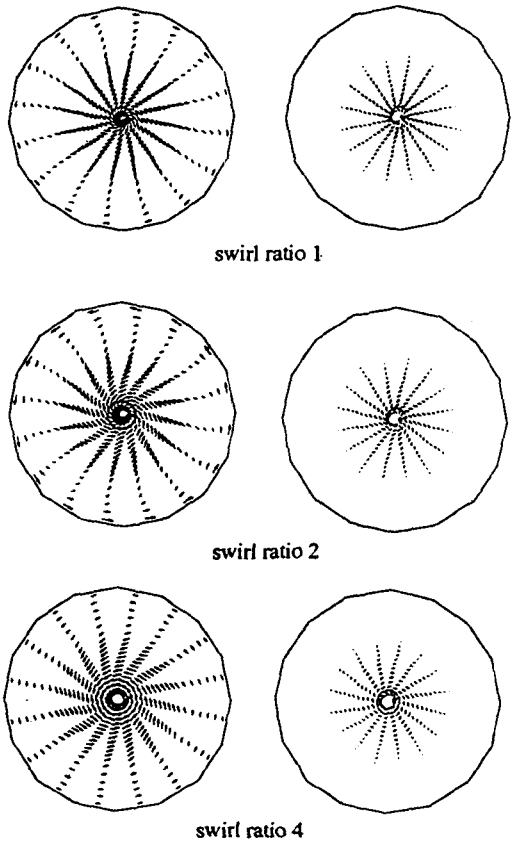

Fig. 5 Velocity fields in the planes of K=12 and K=20
u_{max}=16.78[m/s], v_{max}=16.89[m/s]

motion was caused due to the relative increase of small droplets which had random motion to a much greater extent than the large ones.

The fuel vapor mass fraction. Fig. 6 showed the contours of the fuel vapor mass fraction in the radial-axial plane of J=2 and J=10. As the spray proceeded, the mass of air within the spray increased. The spray droplets evaporated as the air entrainment proceeded. At ATDC 350° and ATDC 360°, as the swirl ration increased the evaporation rate was increased due to the wide dispersion of the spray droplets and the strong interaction between the spray droplets and the gas fields. As the swirl ratio decreased, the fuel vapor increased near the bottom of the piston bowl due to the increased spray droplets

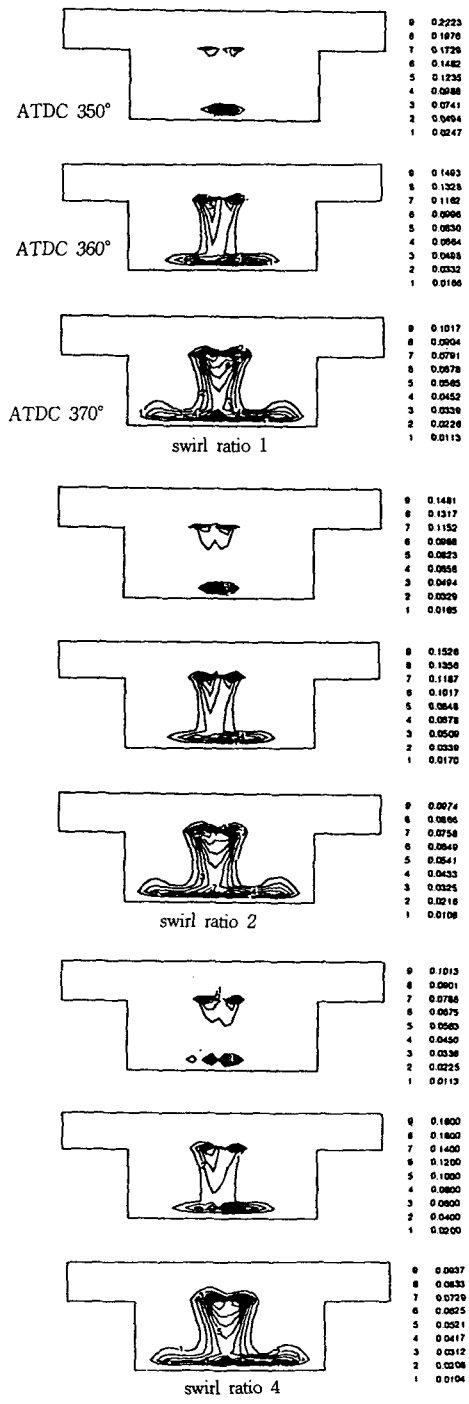

Fig. 6 Fuel vapor mass fractions in the plane J=2 and J=10

impinging on the bottom of piston bowl. Once the spray droplets have penerated the bottom of the piston bowl, the spray droplets was forced to flow tangentially along the bottom wall and then evaporation proceeded. At ATDC 370°, the evaporation rate was little changed for the change of swirl ratios. But in the case of swirl ratio 4 the fuel vapor was much more widely dispersed in the combustion chamber and much less dispersed near the bottom of piston bowl than the other cases.

Fig. 7 showed the contours of the fuel vapor mass fraction in the radial-circumferential plane of K=12. As the swirl ratio decreased the fuel vapor was concentrated in the vicinity of the axis of the combustion chamber due to the spiralling motion as shown in Fig. 5.

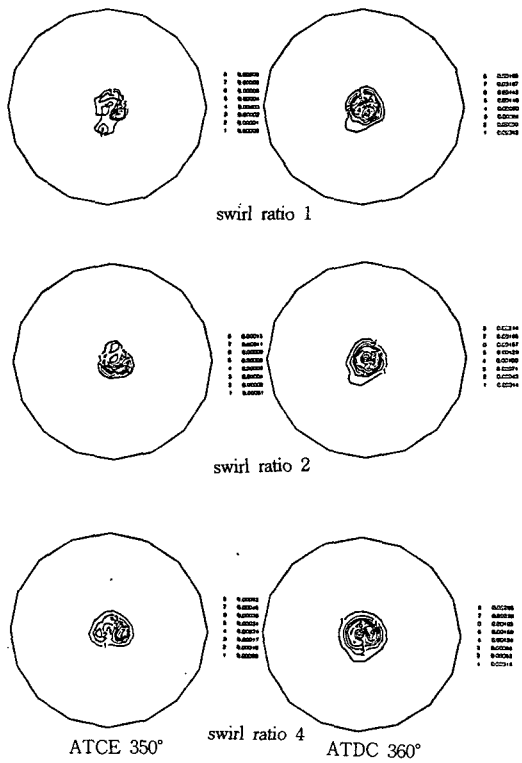

Fig. 7 Fuel vapor mass fractions in the plane K=12

5. CONCLUSION

In this study the governing equations were descretized using a combination of Euler implicit differencing in time and hybrid upwind/central differencing in space. The numerical calculations of the spray characteristics in quiescent condition and the swirl effect on the spray characteristics and the flow fields in a motoring condition of direct engine were performed using the orthogonal curvilinear grid system and PISO algorithm.

The following conclusions were obtained.

1) The results of the calculation showed that the spray tip penetration length were good agreements with the experimental data, except in the early stages of spray. This discrepancy in the early stages of spray was presumably attributed by the assumption that the spray was already atomized at the nozzle exit.
2) A substantial air entrainment into the spray volume where it was accelerated in the direction of injection was emerged and the squish motion was relatively unimportant during the injection periods. In the radial-circumferential planes as the swirl ratio increased there revealed a solid-body rotation, while as the swirl ratio decreased there revealed a spiralling motion and a irregular velocity fields.
3) As the swirl ratio increased the evaporation rate was increased due to the wide dispersion of spray droplets and the strong interaction between the spray droplets and the gas fields. As the swirl ratio decreased, the fuel vapor increased near the bottom of piston bowl due to the increased spray droplets impinging on the bottom of piston bowl.

NOMENCLATURE

- a : area
- C_p : specific heat at constant pressure
- D : diffusivity
- K_d : momentum transfer coefficient
- k_t : thermal conductivity
- m_d : mass of a droplet with diameter D_d
- N_k : number of droplet in parcel k
- P_t : total pressure

$P_{v,\infty}$: vapor pressure far from the droplet
$P_{v,s}$: vapor pressure at the droplet surface
Q : latent heat of evaporation
R : gas constant
W_g : velocity of moving grid
w_R : axial gas velocity relative to the moving grid($=w-W_g$)
u_d, v_d, w_d : droplets velocity in the orthogonal curvilinear coordinate directions ξ, η and ζ
α : heat transfer coefficient
ψ : the dependent variables($=1, u, v, w, f, e_s, k, \varepsilon$)
θ : void fraction
ρ : gas phase density
ξ_d, η_d, ζ_d : droplets position in the orthogonal curvilinear coordinate directions ξ, η and ζ

REFERENCES

1) H.Hiroyasu and T.Kadota, Fuel Droplet Size Distribution in Diesel Combustion Chamber, SAE Paper, 740715, 1974.
2) K.J. Wu, A.Coghe, D.A.Santavicca and F.V. Bracco, LDV Measurements of Drop Velocity in Diesel-type Sprays, AIAA Journal Vol. 22, p. 1263, 1984.
3) R.D. Reitz and R.Diwakar, Structure of High-Pressure Fuel Sprays, SAE Paper, 870598, 1987.
4) J.K. Dukowiz, A Particle-Fluid Numerical model for Liquid Sprays, J.Comput., Vol. 35, No. 2, pp. 229~253. 1980.
5) P.J. O'Rouke, Collective Drop Effects on Vaporizing Liquid Sprays, Los Alomos National Laboratory Report, LA-9069-T, 1981.
6) R.D. Reitz and R.Diwakar, Effects of Drop Breakup on Fuel sprays, SAE Paper, 860469, 1986.
7) G.I.Taylor, The Shape and Acceleration of a Drop in a High Speed Air Stream, The Scientific Papers of G.I.Taylor, ed. G.K. Batchelor, Vol. Ⅲ, University Press, Cambridge, 1963.
8) P.J. O'Rouke and A.A.Amsden, The TAB Method for Numerical Calculation of Spray Droplet Breakup, SAE Paper, 873089, 1987.
9) H.L.Nguyen, H.J Shock, M.H.Carpenter, J.I.Ramos and J.D.Stegman, Numerical Simulation of the Flow Field and Fuel Sprays in an IC Engine, SAE Paper, 870599, 1987.
10) M.H. Carpenter and J.I. Ramos, Mathematical Modeling of Uniflow-scavenged Two-Stroke Diesel Engine, 1987.
11) J.D. Naber and R.D.Reitz, Modeling Engine Spray/Wall Impingement, SAE Paper, 880107, 1988.
12) P.Werlberger and W.P.Cartellieri, Fuel Injection and Combustion Phenomena in a High Speed DI Diesel Engine Observed by Means of Endoscopic High Speed Photography, SAE Paper 870097, 1987.
13) M.Shimoda, M.Shigemori and S.Tsuruoka, Effects of Combustion Chamber Configuration on In-Cylinder Air Motion and Combustion Characteristics of D.I. Diesel Engine, SAE Paper 850070, 1985.
14) Y.H. Chi, J.H. Lee and E.S. Kim, An Experimental Study on Spray Pattern and Droplet Size Distribution of Diesel Spray, J. of Korean SAE, Vol. 14, No. 3, pp.102~108, 1992.
15) W.C. Reynolds, Modelling of Fluid Motions in Engines-An Introductory Overview, in Combustion Modelling in Reciprocating Engines, ed J N Mattavi and C A Amann, Plenum Press, New York, 1980.
16) A.P. Watkins, Three-Dimensional Modelling of Gas Flow and Sprays in Diesel Engines, ed. N.C. Markatos, Computer Simulation for Fluid Flow, Heat and Mass Transfer, and Combustion in Reciprocating Engines, Hemisphere Publishing Corporation, pp. 193~237, 1989.
17) B.E. Launder amd D.B. Spalding, Mathema-

tical Models of Turbulence, Academic Press, London, 1972.
18) R.I. Issa, Solution of the Implicitly Discretised Fluid Flow Equations by Operator-Splitting, J.Comp. Phys., Vol. 62, No. 1, 1986.
19) B.Chehroudi, S.H. Chen, F.V. Bracco and T.Onuma, On the Intact Core of Full-Cone Sprays, SAE Paper 850126, 1985.